ICSV14
Cairns • Australia
9-12 July, 2007

AEROACOUSTIC INVESTIGATION OF A TIP CLEARANCE FLOW

Marc C. Jacob[1], Julien Grilliat[1], Michel Roger[1] and Roberto Camussi[2]

[1]Laboratoire de Mécanique des Fluides et d'Acoustique (LMFA), UMR CNRS 5509, Université Claude-Bernard Lyon I, Ecole Centrale de Lyon,, 69134 Ecully Cedex, France
[2]Mechanical and Industrial Engineering Dept. (DIMI), University 'Roma 3', Rome, Italy
Marc.jacob@ec-lyon.fr

Abstract

Strong unsteady broadband perturbations are found in a tip clearance flow and related to acoustic radiation using standard techniques as well as advanced cross-wavelet analysis. The experiment is carried out on a single non-rotating airfoil in the anechoic wind tunnel facility of the Ecole Centrale de Lyon. The airfoil is placed between two plates into a Mach 0.2 open-jet flow. A strong leakage flow is obtained with a high lift, 5% camber airfoil at a 15° angle of attack. The leakage flow occurs in an adjustable gap between the lower plate and the airfoil tip and the sound radiated into the cross-stream direction is measured in a medium at rest. The influence of the gap size is investigated. PIV measurements are carried out both around the airfoil and in the gap region providing a detailed view of the flow. Unsteady pressure measurements on the airfoil, both in the mid-span region and in the gap region, are combined with single HWA and PIV measurements. A special care is given to placing the probes on the tip of the airfoil, the tip edges and the plate facing the tip. Moreover, 2 sets of probes are installed in the mid-span region both spanwise and chordwise near the trailing edge. An advanced wavelet analysis of the pressure fields allows to identifying the aeroacoustic sources and to relate them to turbulent eddies generated in the gap region.

1. INTRODUCTION

Fan broadband noise appears to be a major sound source of modern aircraft during the approach flights where the engine power and the jet noise are reduced. There are many types of broadband noise sources in fan-OGV secondary flow, not to mention compressor, turbine, and combustion noise that are believed to be either small or immersed in the jet noise. These sources can be decomposed in two families, self noise and interaction noise sources.

Self noise sources are due to flow perturbations generated by the airfoil itself and are converted into sound by the same airfoil. They are mainly located on the rotor and are known as trailing edge noise and tip clearance noise. Perturbations generated at the hub are aerodynamically important but not acoustically since the azimuthal velocity is much lower at the hub; stator self noise exists in principle but is outranged by interaction noise.

Interaction noise sources are due to perturbations advected by the flow onto a blade that are converted into sound when they hit the blade leading edge. Although these perturbations can be of any nature (eg. ingested atmospheric turbulence), they usually originate from another airfoil wake: the main interaction noise source in the secondary flow is the fan-OGV interaction, due to the rotor wakes impinging onto the stator vanes. Since the rotor wakes contain trailing edge perturbations as well as tip clearance perturbations, the interaction noise can also be split accordingly. Another possible interaction noise source is suspected on the rotor tip, the tip–boundary layer interaction that is due to the interaction between the casing boundary layer structures and the fan tip.

Although tip clearance flows have been investigated by many authors, a number of studies [1]–[6] is devoted to axial flow compressors and focused on their aerodynamic performances. However, these studies, as well as recent numerical investigations [7] provide useful information about the unsteady flow features in the tip region. A few studies are concerned with the noise due to axial fan or compressor tip flows. Among these, the early and recent work of Fukano *et al* [8],[9] and the study of Ganz *et al.* [10] provide answers as to the importance of tip clearance noise. Since there are carried out on representative rigs, these works do not relate noise measurements to specific flow perturbations. The latter study does not show tip clearance noise to be a significant noise source of the secondary flow. Nevertheless, among the most recent papers, some even describe attempts to controlling tip clearance noise [11]–[13] by passive devices such as novel tip design, inferring that tip clearance noise is indeed, an important fan noise source.

In order to address this question and to shed a new light onto the flow mechanisms involved in tip clearance noise generation, the present study investigates the tip clearance flow on a single non rotating airfoil both from an aerodynamic and an acoustic standpoint. Thus it is focused on tip clearance self noise and compares it to trailing edge noise. By limiting the study to a single airfoil, the tip clearance flow interaction with an airfoil located downstream is automatically excluded. The choice of a single airfoil allows to carrying out the experiment in an open jet in order to obtain a far field in a medium at rest. A significant tip flow is obtained by loading the airfoil which is highly cambered.

The objectives of the experiment that is briefly reported in the present paper are manifold:

- to classify the tip clearance flow in the hierarchy of fan broadband noise sources,
- to describe its mechanisms with conventional and less conventional tools,
- to provide a database both for modelling and numerical issues.

The experimental set-up is described in section 2, the mean flow in section 3 and typical unsteady flow features in section 4. Finally the sound far field is analysed in section 5.

2. EXPERIMENTAL SET-UP

2.1. Global set-up

The experiment is carried out in the anechoic room (10m×8m×8m) of the Laboratoire de Mécanique des Fluides et d'Acoustique (LMFA), a joint CNRS-ECL-UCBLyon-I laboratory located at the Ecole Centrale de Lyon. Air is supplied by a high speed subsonic anechoic wind tunnel at Mach numbers ranging up to 0.3. The set-up is shown in Figure 1. A NACA5510 profile (5% camber, 10% thickness) with a 200 mm chord and 200 mm span is placed between two horizontal plates. The airfoil is mounted onto a wooden disk, which allows to tuning the angle of attack. The gap is also adjustable, the total height (gap + span) remaining equal to 200 mm. The reference velocity at the exit of the wind tunnel is U_0= 70 m/s, and the turbulence level u'/U_0 is about 0.7%.

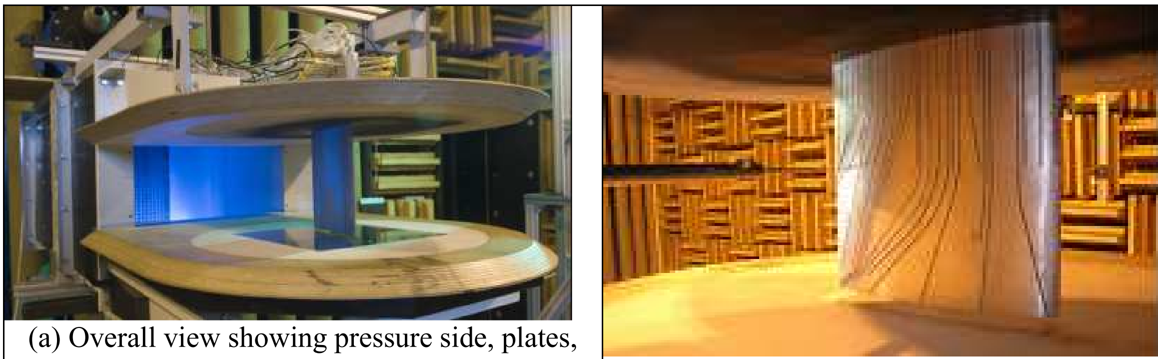

(a) Overall view showing pressure side, plates, remote pressure probes
By Courtesy © CNRS 2006

(b) Detail showing suction side, embedded pressure tubes and hot wire support

Figure 1: Views of experimental set-up

The chord-based Reynolds number is Re_c~930,000. For these inflow parameters, the reference configuration is obtained with a α=15° deg angle of attack, and an h=10 mm gap. The corresponding configuration without gap (h=0) is referred to as the no-gap configuration. The gap is half the gap maximum airfoil thickness and about half the boundary layer thickness (as discussed in section 2). Since the two end plates and the airfoil remain motionless, the gap flow is only induced by the high camber (5%) and angle of attack (15°). This results in a high load and a subsequently significant gap flow.

2.2. Co-ordinate system

The coordinate system is bound to the profile is useful to locate the wall pressure probes. The origin O_g is located at the leading edge tip: the x axis is following the aerodynamic chord pointing from the leading to the trailing edge; the z axis follows the span-wise direction from the gap to the upper plate and the y axis is normal to the chord, pointing from the pressure to the suction side.

2.3. Measurements

Measurements referred to in this paper include:

- both single and cross-wire anemometry to characterize the incoming flow and the wake
- PIV measurements in the vicinity of the airfoil at various spans, including the tip clearance gap, with a La Vision system and two fast high resolution cameras (1280×1024 pixels each),
- steady and unsteady pressure measurements on the airfoil and the lower plate, including the gap: the sampling rate is 64 kHz and the time series are long enough to perform 500 averages of 8192 point FFT's; this is enough to obtain a statistical error of less than 1% on the coherence between 2 signals; the measurements are carried out with a remote microphone technique described by Roger and Perennes [14]; the sensors used are B&K type 4935 ICP ¼" microphones that are pre-amplified by a PXI system; they are connected to the wall measurement pinholes via small capillary tubes;
- far field measurements are performed at about 1.5 m from the airfoil leading edge with two B&K type 4191 ½" microphones that are turned around the airfoil, in far field conditions above ~250 Hz.

3. MEAN AND RMS FLOW

3.1. Surrounding jet flow

First, it is checked with single Hot Wire Anemometry that the airfoil is indeed in the potential core of the jet. The cross-stream velocity profile half a chord upstream of the airfoil is found to be uniform within 5% at mid-span. The jet shear layers remain ~ ½ to 1 chord away from the airfoil in all directions. ½ chord upstream of the airfoil, a δ~ 18 mm boundary layer with a displacement thickness δ^*~1.4 mm develops on the lower plate. The fluctuation level is very low in the jet core, 0.7% ±0.05%, but climbs up to 8% in the bottom boundary layer.

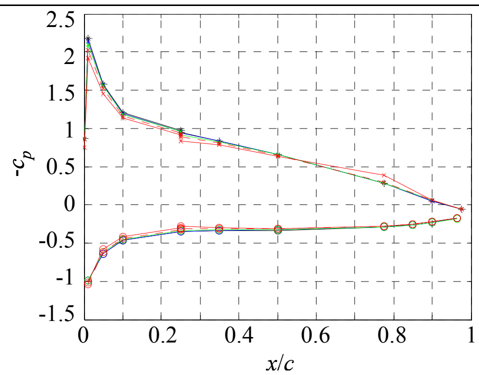

Figure 2: Gap influence onto mid-span pressure at 70 m/s: no gap (black); h[mm]=1(blue); 2(green); 5 (red dash); 10(red continuous)

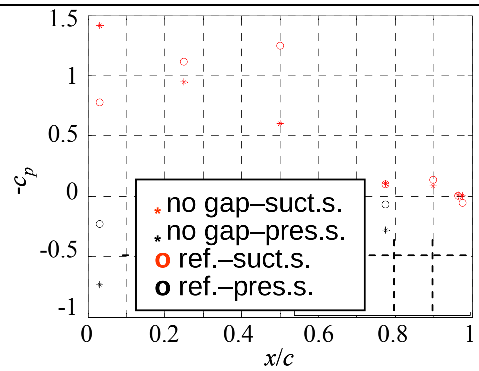

Figure 3: Pressure coefficient at the tip edge: with gap (circles) and without gap (stars) – suction side (black) and pressure side(red)

In the mid-span region the flow is not significantly affected by the tip clearance flow as shown on Figure 2, where the pressure coefficient along the mid-span chord is plotted for various gap heights from h= 0 to 10 mm. This is confirmed by velocity measurements in the same region. In the gap region however, the flow is completely modified by the tip clearance flow, as illustrated on Figure 3 where the chordwise pressure coefficient obtained at the tip edge is plotted both with and without gap. Besides the fact that pressure distributions of the two configurations are quite different in this region, it can be observed that for the reference configuration, the suction at mid-chord is significantly increased with respect to the no-gap case.

This corresponds to the region where the gap flow is strongest in the reference case as illustrated by the PIV mean velocity chart on Figure 4(a). Indeed, the pressure difference between the to airfoil sides generates a very strong jet-like flow that exits the suction side in a cross-stream direction near x/c~0.5. There it is deviated by the main flow and rolls up into the tip vortex which is evidenced on Figure 4(b) by the two high perturbed regions. One region is in the vicinity of the airfoil suction side and could be a significant noise source. However, the gap itself is not the most turbulent region. This behavior has also been described in other studies (e.g. [5], [6]). The velocity of this side jet reaches ~1.5 times the free stream velocity. These features are unchanged when the gap except for the intensity of the gap flow which vanishes as the gap is reduced.

The most spectacular changes occur if the angle of attack is modified: as it increases, the gap jet moves upstream: it occurs in the downstream quarter of the airfoil at α=5° and almost at the leading edge when α=18°. Moreover, it was found that the gap flow scales with the free stream velocity, which means that the physics of this flow are not really velocity dependent.

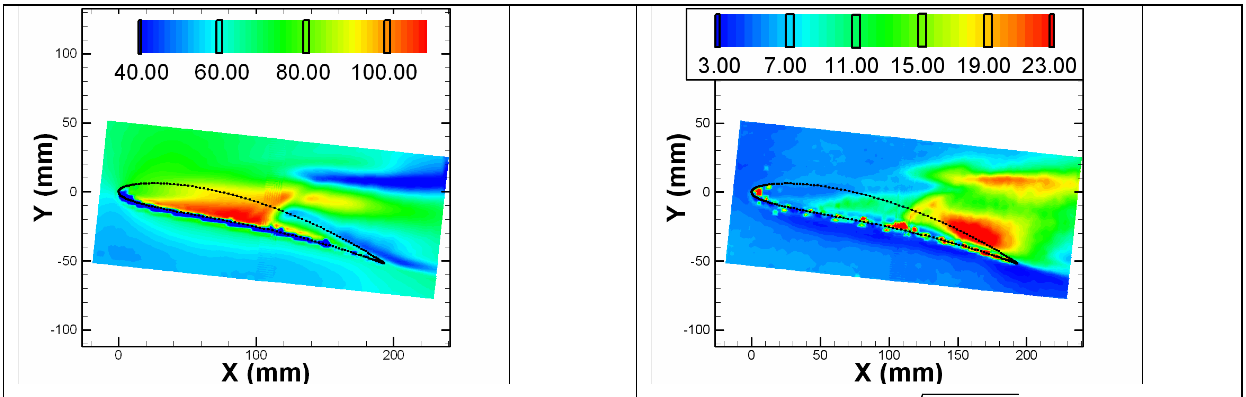

(a) |**V**| (b) $\sqrt{u'^2+v'^2}$

Figure 4: PIV velocity field in the gap (at z=7mm) for the reference configuration (h= 10 mm, α= 15°, U_0=70 m/s): mean velocity modulus (a); 2D – turbulence level $\sqrt{u'^2+v'^2}$ (b) – scales are given in m/s.

4. FLUCTUATING FLOW

As it could be expected, this skewed side flow generates strong unsteady perturbations that are candidate noise sources.

4.1. Wall pressure spectra

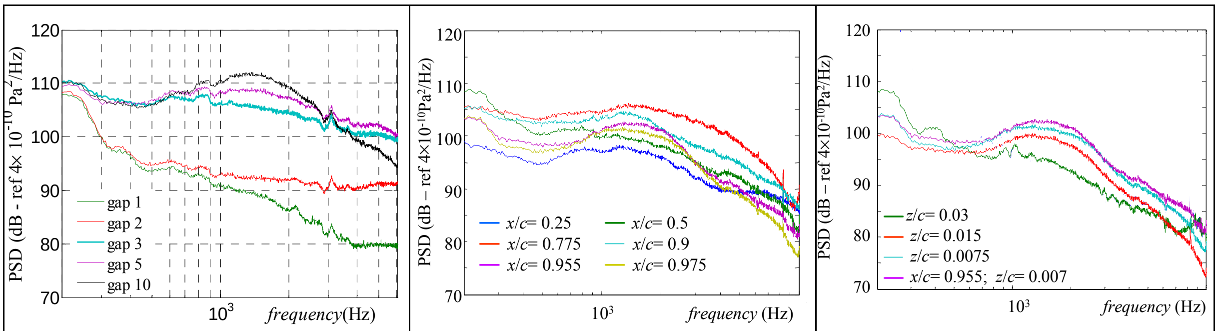

(a) tip probe in gap x/c=0.775 (b) tip edge (suction side) (c) tip-TE corner (suction side)

Figure 5: wall pressure spectra in the gap and near the gap on suction side in reference configuration

On Figure 5, typical spectra from the suction side on the tip edge and the trailing edge-tip corner are traced on plot (b) and (c) respectively. Plot (a) compares data from several gaps obtained on the tip at ¾ chord: the gap flow becomes highly unsteady when h exceeds 2 mm, this is an aspect ratio smaller than 10 between the airfoil thickness and h in the region of the side jet. It can also be observed that the unsteady gap flow is responsible for a medium frequency hump (~0.5–3 kHz). Similar features are also found on velocity spectra in this region.

4.2. Coherence

Cross-coherences from a set of span-wise distributed probes near the tip–T.E. is shown on Figure 6 (a) where η denotes the probe spacing in (mm). The coherence length is about 6 mm at 1.5 kHz and falls down to ~1 mm at 4 kHz. The coherence between a hot wire located near the T.E. at (*x*/*c*, *y*/*c*, *z*/*c*) ~ (0.95; 0.1; 0) and pressure probes implemented into the bottom plate in the same region are plotted on (b). The probe locations are sketched on plot (c) and their cross-stream co-ordinates *y*/*c* are given in the legend of plot (b). The upstream probe is located on the plate at *x*/*c*=0.775 in the middle of the gap. The span-wise coherence is high at low and medium frequencies (even for probes that are far from the wall) corresponding to the hump of the spectra shown in Figure 5.

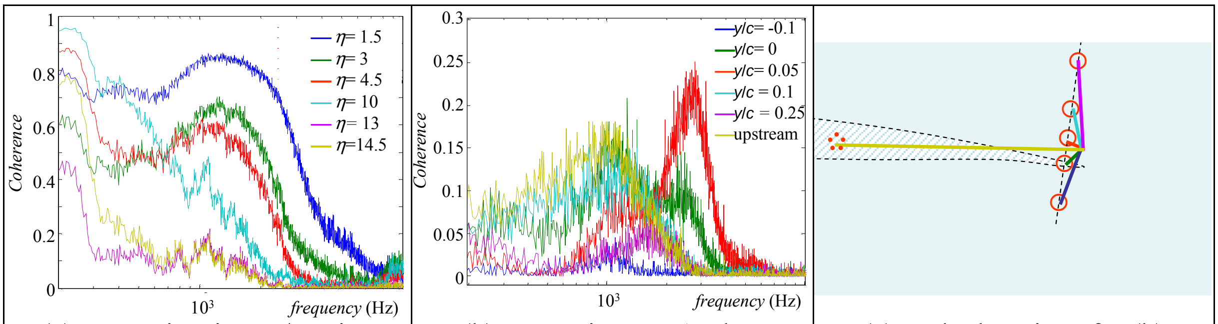

(a) span-wise tip-TE/suction (b) span-wise HWA-plate (c) probe locations for (b)

Figure 6: span-wise pressure coherence at TE-tip corner (suction side) (a) and HWA-pressure coherence at bottom plate, HWA located near TE-suction side 5 mm above microphone *y*/*c*=0.05 (b). (reference configuration), sketch of probe locations (c).

4.3. Wavelet analysis

The wavelet analysis has many common points with Fourier analysis, the main differences are that a family of wavelets (the Battle-Lemarie wavelets in the present study) replaces the complex exponentials. The result of a decomposition on this family of transient functions are wavelet coefficients that depend both on time and on a time scale *r* (the time scale of the wavelet) whose inverse 1/*r* is the wavelet equivalent of the frequency. On the basis of this wavelet transform, it is possible to carry out cross-wavelet analyses in order to correlate wavelets from 2 signals. The purpose of using wavelets is to obtain a sharper description of transient flow phenomena (*e.g.* coherent structures in turbulent flows such as turbulent boundary layers). In particular the LIM (local intermittency measure) and its two-signal counterpart, the cross-LIM, generalize the concept of energy and of cross-spectrum respectively. Peaks of *LIM* represent large contributions of a signal's variations to its overall power level. Therefore the *LIM* amplitude at a selected scale *r* can be thresholded in order to select events responsible for the largest fluctuations of the analyzed signal and to determine how they are distributed in time. Once the events have been selected and localized in the time, a conditional average of the original signal is performed. This auto-conditioning procedure leads to an ensemble averaged time signature of the fluctuations, which represents the most probable shape of the most energetic structures which are hidden in the original chaotic signal. The original method was introduced in 1997 by Camussi and Guj [15]. In the present study, velocity measurements using a single probe hot wire anemometer (HWA) have been conducted simultaneously to the wall pressure measurements in several configurations. The example shown here is obtained from simultaneous PIV/pressure measurements performed in the reference configuration. The conditioning method explained above is applied to the PIV/wall-pressure data: first, aerodynamic events correlated to large localized pressure peaks at the wall of the airfoil. Second, the conditional average is performed on those PIV snapshots that are acquired simultaneously with the selected pressure events. An example of this approach is shown on Figure 7 where a snapshot is shown on plot (a), and the conditionally averaged PIV on plot (c). The selection event is a high frequency one shown on plot (b). Plot (c) shows that the flow structures responsible for these high frequency events occur about a ¼ chord upstream of the probe in the gap: this is the region where the highest gap flow velocities are observed and subsequently the strongest gap perturbations are found. The Cross-LIM analysis of pressure-pressure of pressure-HWA measurements also allows to reconstruct time signatures and phase speeds of selected events, which of course is not accessible with non time-resolved PIV.

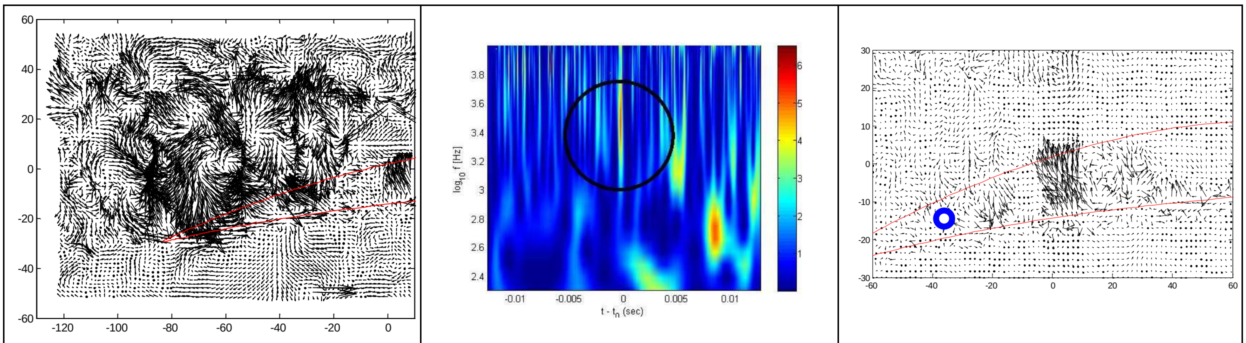

(a) instantaneous velocity (b) high frequency event(circle) (c) conditional average

Figure 7: Example of conditionally averaged PIV measurement in the reference configuration: the event is selected on the gap probe located at x/c=0.775 on the airfoil tip (blue circle on plot (c))

5. SOUND FIELD

The far field spectra at 1.5 m from the airfoil and an angle of 85° are plotted on plot (a) of Figure 8: they show the gap noise is of the same order as the classical TE noise, higher at some frequencies (difference >+3dB), lower at others (< 3dB) or negligible (< 0dB). If the difference is large enough (>0dB), the PSD of the T.E. noise can be subtracted from the overall T.E. and gap PSD, giving an estimate of the gap induced noise. The result is summarized on plot (b) for all observation angles.

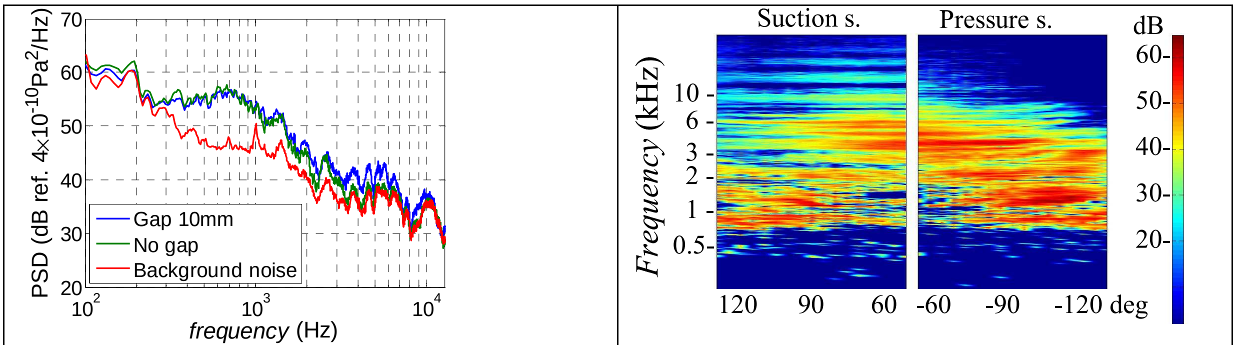

(a) far field spectra at 85 (b) tip clearance noise : spectrum vs. obs. angle

Figure 8: far field: comparison of reference, no gap, and no-airfoil configurations at 70m/s in 85° observer direction (a); reconstructed pure gap noise frequency-directivity diagram.

Two sources are identified. One is a medium frequency (0.7–2 kHz) corresponding to the humps observed in the pressure spectra that radiates into the upstream directions. The other is a higher frequency source (3–7 kHz), probably related to the high frequency events discussed in the wavelet analysis, that radiate when they pass the tip edge or the TE. This source radiates more into the downstream arc. It is comparable and even louder than the sum of the TE and the background noise.

6. CONCLUSIONS & AKNOWLEDGEMENTS

This experiment provides a large data base about tip clearance flow of a single airfoil. Only a few typical results are presented here due to the large amount of available data. Many features of the tip clearance self noise source have been identified with a variety of tools, the jet-like clearance flow feeding the tip vortex, the spectrum of the tip flow perturbations associated to coherent structures. A medium frequency contribution recognizable on all flow spectra is found to radiate into the upstream directions especially on the pressure side, whereas a high frequency contribution is observed in the downstream arc. The latter is might be due to high frequency eddies generated at the tip and amplified by the lower TE-corner. This quite unique free-stream tip flow experiment not only allows an aeroacoustic study but also provides a data base for CFD and analytical modelling: indeed, coherence length and convection velocities and other quantities of interest for modellers could be derived from this data set.

This work is funded by the E.U. project PROBAND No. AST4-CT-2005-012222 on fan broadband noise. The authors wish to thank Mr. Jondeau for his help in the experiment.

REFERENCES

[1] J.P. Bindon, "The measurement & Formation of Tip Clearance Loss", *Journal of turbomachinery*, **111**, 257-263, (1989).

[2] M. Inoue and M. Kuroumaru, "Structure of Tip Clearance Flow in an Isolated Axial Compressor Rotor", *Transactions of the ASME*, **111**, 250-256, (1989).

[3] J.A. Storer and N.A. Cumpsty, "Tip Leakage Flow in Axial Compressors", *Transactions of the ASME*, **113**, 252-259, (1991).

[4] B. Lakshlinarayana, M. Zaccaria and B. Marathe, "The Structure of Tip Clearance Flow in Axial Flow Compressors", *Transactions of the ASME*, **117**, 336-347, (1995).

[5] Tang G.: *Measurements of the Tip-gap Turbulent Flow Structure in a Low-speed Compressor Cascade*, Ph.d. thesis, Faculty of the Virginia Polytechnic Institute and State University, (2004).

[6] Intaratep N.: *Formation and Development of the Tip Leakage Vortex in a Simulated Axial Compressor with Unsteady Inflow*, Ph.d. thesis, Faculty of the Virginia Polytechnic Institute and State University, (2006).

[7] D. You, M. Wang, P. Moin and R. Mittal, "effects of tip-leakage flow in a turbomachinery cascade", *Physics of Fluids*, **18**, on-line manuscript n°105102, (2006).

[8] T. Fukano and Y. Takamatsu, "The effects of tip clearance on the noise of low-pressure axial and mixed flow fans", *Journal of Sound and Vibration*, **105**, 291-308 (1986).

[9] T. Fukano and C. Jang, "Tip clearance noise of axial flow fans operating at design and off-design condition", *Journal of Sound and Vibration*, **275**, 1027-1050 (2004).

[10] Ganz U.W., Patten T.J., Scharpf D.F. & Joppa P.D.: *Boeing 18-inch fan rig broadband noise test*. NASA CR-1998-208704, (1998).

[11] J.W. Bae, K.S. Breuer and C.S. Tan, "Active control on tip flow in axial compressors", *Journal of turbomachinery*, **127**, 352-362, (2005).

[12] M.R. Khourrami and M. Choudari, "A novel approach for reducing rotor tip-clearance induced noise in turbofan engines", *AIAA-paper***2001-2148,** (2001).

[13] A. Corsini, B. Perugini, F. Rispoli, A.G. Sheard and I.R. Kinghorn, "Experimental and numerical investigation on passive devices for tip clearance induced noise reduction in axial flow fans", *7th European Conference on Turbomachinery* (ECT-7), 5-9 March 2005, Athens, Greece.

[14] M. Roger and S; Perennes, "Aerodynamic noise of a two-dimensional wing with high-lift devices", *AIAA-paper n°***98-2338**, (1998).

[15] R. Camussi and G. Guj, "Orthonormal wavelet decomposition of turbulent flows: intermittency and coherent structures", *Journal of Fluid Mechanics*, **348**, 177-199, (1997).